ACS Catalysis

Research Article

pubs.acs.org/acscatalysis

Gold Nanoparticles Supported on Carbon Nitride: Influence of Surface Hydroxyls on Low Temperature Carbon Monoxide Oxidation

Joseph A. Singh,[†] Steven H. Overbury,[‡] Nancy J. Dudney,[†] Meijun Li,[‡] and Gabriel M. Veith*[,†]

[†]Materials Science and Technology Division and [‡]Center for Nanophase Materials Sciences, Oak Ridge National Laboratory, Oak Ridge, Tennessee 37831, United States

Supporting Information

ABSTRACT: This paper reports the synthesis of 2.5 nm gold clusters on the oxygen free and chemically labile support carbon nitride (C_3N_4). Despite having small particle sizes and high enough water partial pressure these Au/C_3N_4 catalysts are inactive for the gas phase and liquid phase oxidation of carbon monoxide. The reason for the lack of activity is attributed to the lack of surface −OH groups on the C_3N_4. These OH groups are argued to be responsible for the activation of CO in the oxidation of CO. The importance of basic −OH groups explains the well documented dependence of support isoelectric point versus catalytic activity.

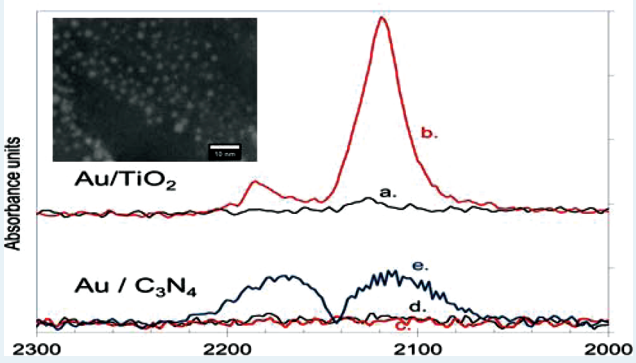

KEYWORDS: *gold, CO oxidation, carbon nitride, hydroxyls, sputtering*

INTRODUCTION

Of all the variables reported to influence the activity of supported gold nanoparticles for the oxidation of carbon monoxide, (i.e., particle size, oxidation state, electronic structure, and synthesis methodology), the choice of support material plays one of the most critical, but undefined roles.[1−6] Nearly all studies of gold-support interactions have focused on oxygen containing supports, for example, TiO_2, Fe_2O_3, CeO_2, MgO, $LaPO_4$, $Mg(OH)_2$, $La(OH)_3$, and so forth.[7] Under ambient conditions the surfaces of typical metal−oxygen support materials are terminated by hydrogen and coated with physisorbed coordinating water molecules.[8−13] The surface hydration/protonation are often strong enough that the surface OH species are observed on bulk metal oxides like TiO_2 under ultrahigh vacuum (UHV) conditions.[14] This water is the reason samples need to be degassed before performing gas physisorption Brunauer−Emmett−Teller (BET) surface area measurements. These surface OH groups can be removed by applying aggressive processing conditions including heating (>800 °C) and ion bombardment under UHV conditions.[15] There is a growing body of evidence that these surface $-OH/H_2O$ species may play the critical role in the formation of structurally stable and catalytically active bulk gold catalysts.[16]

The first indication of the importance of water or OH were from gas phase CO oxidation studies which showed at least an order of magnitude increase in activity and catalyst lifetime by increasing the water concentration in the reaction feed.[17−20] In 2003 Costello et al. reported a model for catalytic activity where Au−OH moieties created by pretreatement in H_2/H_2O streams activated the gold particles for CO oxidation.[21] In 2004 Sanchez-Castillo et al. showed that gold nanorods grown from silver seeds were 5 times more active for CO oxidation at very basic conditions (pH 13) which they attributed to the OH groups in solution.[22] Later Ketchie and Davis showed a 50 fold increase in the aqueous phase oxidation of CO of gold clusters supported on carbon by increasing the pH from 0.3 to 13.[23] These same clusters were inactive for gas phase CO oxidation.[23] Later in 2008 Moreau et al. postulated that the increase in activity for gold catalysts on Ce based oxides may be attributed to hydroxyl groups acting catalytically for CO oxidation.[24] Previous investigations of support effects on the reactivity of gold catalysts have noted that clusters supported on metal hydroxides like $Mg(OH)_2$, $Be(OH)_2$, and $La(OH)_3$ are more reactive at lower temperatures (<196 K) than those supported on materials like TiO_2, which have intermediate values of isoelectric points (IEP).[25] Furthermore all these catalysts are more active than materials supported on acidic supports like SiO_2 (IEP ∼ 2) and WO_3 (IEP ∼ 1) despite similar gold particle sizes.[25−27] The trends in support basicity and activity indicate that the presence of strongly basic OH groups on the surface of a support material results in high activity toward gas phase CO oxidation.

We recently demonstrated that adding hydroxyls to the surface of TiO_2 supports during the synthesis of a gold catalyst resulted in a 2 orders of magnitude increase in catalytic activity for the gas phase oxidation of CO over oxidized gold particles (1.2−1.3 nm), compared to TiO_2 supports without hydroxyls.[28] A similar (though smaller in magnitude) enhancement in

Received: February 13, 2012
Revised: March 29, 2012
Published: May 14, 2012

   dx.doi.org/10.1021/cs3001094 | ACS Catal. 2012, 2, 1138−1146

activity was observed for metallic gold particles (1.3 nm) with the formation of strongly bound hydroxyls.[14] The addition of strongly bound OH groups resulted in structurally stable gold clusters; without the OH the clusters rapidly migrated at room temperature and coalesced into large 20 nm gold particles.[14] Subsequent work by several groups has also showed a similar increase in the catalytic activity of gold catalysts by adjusting the hydroxyl species on TiO_2[29] or SiO_2[30] supports. In addition, several papers have reported a similar increase in nanoparticle stability through the introduction of strongly bound OH groups.[31−33]

The unanswered and critical question from all of these studies is: What role do the OH's play in the resulting catalytic mechanism? Do they facilitate the activation of CO or O_2 or both? To address these questions we prepared gold clusters on a nonoxide support that does not readily form hydroxyls and whose electronic properties are distinctly different from oxide supports; graphitic carbon nitride (g-C_3N_4). g-C_3N_4 will not oxidize at ambient or typical CO oxidation reaction condition. Instead the surface of the material is terminated with Lewis type basic N−H groups making it an ideal platform to compare with the typical Brönsted type functionality (OH) found on oxides. g-C_3N_4 is a unique electron rich semiconducting organic compound that adopts a graphite-like structure composed of C−N sheets and is thermally stable up to 500 °C in air.[34,35] Graphitic carbon nitrides have been shown to be good catalysts for oxygen activation in numerous fuel cell studies[36−39] and other catalytic studies.[38] Finally, reports of gold catalysts have indicated that donation of electron density from the support to gold at defect sites, predicted to be common on semiconductor supports, leads to increased activity for low temperature CO oxidation.[40−42] The semiconducting g-C_3N_4 with aromatic bonding is an interesting candidate for exploring these electronic effects. The combination of electronic, surface, and oxygen activation properties of this material makes it possible to probe the effect of surface Brønsted-type protons on the activation of CO molecules.

EXPERIMENTAL METHODS

Synthesis. Graphitic carbon nitride (g-C_3N_4) powder was prepared by thermally decomposing cyanamide (99%, Aldrich Chemistry) at 550 °C in an alumina crucible for 2 h under flowing nitrogen gas (Air Liquide, 99.995%). The resulting powder was ground in a mortar and used in subsequent studies. A portion of the g-C_3N_4 powder was treated under alkaline conditions to try to increase its basicity and add surface hydroxyls. Following a previously reported procedure,[14] 5 g of g-C_3N_4 was dispersed in 380 mL of 18 MΩ deionized (DI) water and constantly stirred using a 2″ Teflon coated stir bar in a 600 mL beaker. Approximately 0.5 mL of 0.1 M HCl, prepared by diluting concentrated HCl (Mallinckrodt), was added to simulate chloride ions present in auric acid solution based techniques. A 0.2 M solution of NaOH was prepared from solid NaOH (97.0%, Alfa Aesar-Na_2CO_3 impurity) and used to adjust/maintain a pH of 10 while the mixture was stirred at 57 °C for 90 min. The suspension was centrifuged and washed eight times using deionized water, dried in a vacuum oven overnight, and then analyzed for residual sodium from the NaOH using XPS. The powder was washed and centrifuged three more times and dried in a vacuum oven for 150 min. XPS measurements showed ∼1 atomic percent residual Na surface content that could not be removed by washing with hot deionized water. Surface acidity/basicity was estimated by measuring the equilibrium pH, with an Orion pH electrode, of approximately 15 m^2 of material in 25 mL of deionized water degassed by boiling and cooled to room temperature under flowing N_2.

To prepare the catalysts, atomic gold species were deposited on the powders using a previously described direct current magnetron sputtering technique.[43] g-C_3N_4 powder was placed in a stainless steel cup with two 1″ Teflon coated stir bars. The stainless steel cup was rotated to agitate the powder and ensure homogeneous gold nanoparticle deposition. A gold target (Refining Systems, 99.95%) was sputtered in an argon (Air Liquide Research grade, 99.9995%) plasma at an applied power of 13 W for 30 min. For comparison a 0.66 wt % Au on carbon catalyst (Calgon Carbon)[23] was prepared using the same method and evaluated in the liquid phase reaction (T = 16 °C).

Catalytic Testing. Carbon monoxide oxidation tests were performed to evaluate catalytic activity using a custom-built flow reactor. Approximately 0.25 g of catalyst was loaded in a quartz U-tube (4 mm inner diameter) and supported by quartz wool. A mass flow controller (Smart-Trak, Sierra Instruments) was used to deliver a constant flow rate of 1 CO: 6 O_2: 93 He (± 2%, Airgas). Gas phase water content, 49 ppm H_2O, was determined using a dewpoint sensor located after the reaction bed (Vaisala DRYCAP). Temperatures were measured using a K-type thermocouple resting on the exit side of the catalyst bed. A gold on TiO_2 reference catalyst (World Gold Council #02-05, Sued-Chemie, powder sample BET SA = 73 m^2/g) was used to compare catalytic activity and surface chemistry. Changes in CO, O_2, and CO_2 concentrations were measured using an Ametek Dymaxion mass spectrometer. Liquid phase CO oxidation was performed in 30 mL of a 1 M NaOH solution in a 50 mL Parr Autoclave system (0.20 g Au/C_3N_4 catalyst) with a gas entraining system in both batch and constant flow modes following the procedure described by Ketchie and Davis.[23] Briefly, the system was flushed and pressurized to 10 psig with He and monitored by a pressure gauge and the mass spectrometer to make sure the cell was not leaking to air. After confirming the cell was not leaking it was charged with the same CO, O_2, and He mixture used for the gas phase studies to 10 psig then sealed to form a batch reactor. A small capillary attached to the Ametek Dymaxion mass spectrometer was inserted into the reactor, through a septum, and used to monitor changes in the CO and O_2 concentrations as a function of time. The volume of gas sampled, relative to the total volume of the cell was so small there was no decrease in cell pressure over 30 min. CO_2 production was not directly determined because CO_2 reacts with Na in the NaOH solution to form Na_2CO_3.

Characterization. Thermogravimetric analysis (TGA) was carried out on a NETZSCH STA 409 PC instrument. Samples were loaded in alumina crucibles and measurements performed in air, heating at 10 °C/minute. Powder X-ray Diffraction (PXD) measurements were performed using a Siemens D5005 X-ray Diffractomer with a CuK_α source and Ni filter. Samples were scanned as loose powders on glass slide sample holders. Fourier Transform Infrared (FTIR) spectroscopy data was measured using Bio-Rad 575c FTIR spectrometer. g-C_3N_4 samples were ground with KBr (KBr crystals, Allied Chemical) to form 8 wt % mixtures, then pressed at 10,000 kg into 0.16 g pellets and measured in the FTIR spectrometer after purging the chamber with dry CO_2 free air for a minimum of 20 min. Nitrogen physiosorption measurements (BET) measurements were performed using a Quantochrome Autosorb 1C instrument.

dx.doi.org/10.1021/cs3001094 | ACS Catal. 2012, 2, 1138−1146

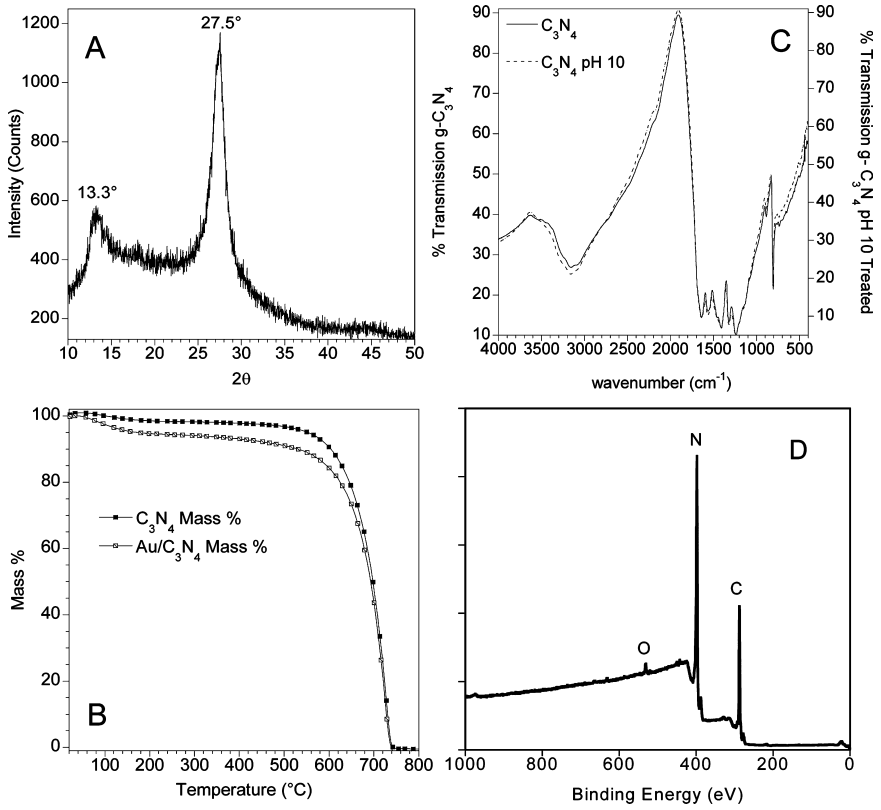

Figure 1. (A) PXD of g-C3N4, (B) TGA measurements in air of C_3N_4 and Au on C_3N_4,(C) comparison of FTIR spectra of g-C3N4 before and after pH 10 treatment, and (D) XPS survey data of C_3N_4.

Samples were heated to 300 °C under vacuum for a minimum of 20 h prior to measurement.

Surface chemistry was determined using a PHI 3056 X-ray Photoelectron Spectroscopy (XPS) spectrometer with an Al source in a 2×10^{-10} Torr vacuum chamber. Samples were pressed into Indium foil (Alfa Aesar), and the foil was attached to the sample holder using carbon tape (Nisshin E. M. Co. Ltd.). High resolution scans were taken with 5.85 eV pass energy, 0.05 eV energy step, and 100 repeats to reduce instrument noise. Charging effects were compensated for by shifting binding energies based on adventitious carbon 1s peak (284.8 eV). Peak fits and atomic surface concentration analysis was performed using PHI Multipack software. Error in peak fits was estimated to be ±0.1 eV. Electron microscope images were collected using a Hitachi HD2000 Scanning Transmission Electron Microscope (STEM) operating at 200 kV and a Hitachi HF3300 STEM operating at 300 kV. Particle sizes were determined by analyzing the STEM images with ImageJ.[44] Gold loadings were determined using Inductively Coupled Plasma (ICP) optical emission spectroscopy (Thermo Jarrell Ash IRIS spectrometer). An approximately 0.05 g sample was soaked in 5 mL of freshly prepared Aqua-Regia in a test tube for 1 h and then sonicated for 30 min. The test tubes were centrifuged, and the supernatant solution decanted and saved. The remaining powder was then mixed with deionized water and centrifuged, again decanting and saving the supernatant solution. XPS was used to confirm the total dissolution of gold.

Information about CO adsorption was obtained using diffuse reflectance FTIR (DRIFTS) spectroscopy in a Nicolet Nexus 670 FTIR spectrometer using a MCT/A detector with a spectral resolution of 4 cm^{-1}. A temperature controlled DRIFTS cell having a volume about 6 cm^3 (Pike Technology) attached to a pulsed gas handling system was used. After the desired pretreatments, a background spectrum was collected from the sample using 256 scans and 4 cm^{-1} resolution. DRIFTS spectra were obtained by subtracting the background spectrum from subsequent spectra. Prior to data collection, as-synthesized Au/C_3N_4 were pretreated in He flow prior to introducing pulses or a steady flow (25 cm^3 /min) of 2% CO/2% Ar/He.

RESULTS

After preparation the g-C_3N_4 has a yellow-orange color consistent with what has been shown previously[35,45−47] and an equilibrium pH of 6.0 indicating that it is slightly acidic. PXD data reveals the presence of peaks at 13.3° and 27.5° 2θ (Figure 1a) corresponding to a graphite-like structure with interplanar spacing of approximately 0.33 nm in agreement with previous reports.[35,45−47] The average grain size was estimated to be 7 nm using the Debye−Scherrer Equation ($K = 0.9$).[48] Nitrogen BET measurements of the as-prepared C_3N_4 showed a BET surface area of 13.4 m^2/g with no microporosity as evidenced by the t-method (de Boer). TGA measurements in air (Figure 1b) indicate that the g-C_3N_4 is thermally stable up to 500 °C. Figure 1d shows survey XPS data for the as prepared carbon nitride. There is a small concentration of oxygen species (0.4 at%) on the surface of the carbon nitride, Table 1. This low concentration of surface oxygen is unusual for nitride materials exposed to air; nitrides, for example, BN, TiN, Si_3N_4 usually react rapidly with ambient oxygen to form a surface oxide.[49] Elemental analysis from the XPS data revealed that the surface was primarily composed of C (41 at%) and N (59 at%) which is consistent with the C_3N_4 stoichiometry. FTIR spectra (Figure 1c) of the carbon nitride is consistent with previously

dx.doi.org/10.1021/cs3001094 | ACS Catal. 2012, 2, 1138−1146

Table 1. Summary of Atomic Surface Concentrations from XPS Measurements, Weight Loadings from ICP Spectroscopy, and Au Particle Sizes from STEM Imaging of the Catalysts and Their Respective Supports

	Au/C_3N_4	C_3N_4	Au/C_3N_4 pH 10 treated	C_3N_4 pH 10 treated
Au median particle diameter (nm)	2.5		2.8	
% dispersion[b]	55.1		51.1	
catalytic onset temperature (°C)	230		320	
space velocity[a]	7500		5000	
% Au weight loading	0.21		0.39	
surface concentrations (atomic %)				
C	38	41	39	41
N	52	59	54	57
O	2	0.4	0.1	1
Au	8.4		6.4	
Na			0.8	0.6
C/N	0.73	0.69	0.72	0.72

[a]Space velocity = (volume gas/hour)/(volume of catalyst bed). [b]Dispersion calculated assuming hemispherical gold cluster. If particle was flatter, the dispersion will be slightly higher.

reported results.[50,51] The broad band at 3155 cm^{-1} is attributed to stretching modes of NH and NH_2. The band at 1313 cm^{-1} corresponds to C(sp^2)-N stretching, and the band at 1635 cm^{-1} corresponds to C(sp^2)=N stretching modes.[51] The 807 cm^{-1} band corresponds to s-triazine ring vibration modes.[52,53] The 1235 cm^{-1} and 1319 cm^{-1} bands correspond to C-NH-C units found in melem.[50,53] There were no observed O−H vibrational bands in the FTIR data which is consistent with the low oxygen functionality observed in the XPS data.

Figures 2 show the C, N, and O XPS data collected for the as prepared and pH 10 treated C_3N_4 respectively. N1s XPS data for the supports shows the presence of C−N=C and N-$(C)_3$ functionalities (398.3 and 400.3 eV respectively).[35,50] The ratio of C−N=C to N-$(C)_3$ (Table 2) roughly agrees with the expected ratio of 3:1 based on the theoretical structure with the untreated g-C_3N_4 being 4.0:1 and 3.3:1 for the pH 10 treated. This deviation may be explained based on the presence of the N−H and N=O peak at 404.3 eV (Figure 2) which indicates the presence of partially condensed tri-s-triazines or surface primary amines, leading to structural defects on or near the surface which account for <4% of surface sites.[35] XPS data collected for the carbon species was consistent with the formation of C−N functionalities (288 eV) in the melem base structure. Low concentration C1s peaks were observed at 284.8 eV because of adventitious C−H from hydrocarbon contamination and 293.5 eV due carbon in a highly oxidized carbon species (C^+). The O1s data shows a single O species with a binding energy of 530 eV which is attributed to the formation of C=O moieties.[54]

Figure 3 (top left) shows a representative STEM image of the gold clusters grown on the as-prepared C_3N_4; particle size histogram are shown in Figure 3 (lower left). There is a dense homogeneous distribution of gold nanoparticles with an average particle size of 2.5 nm, Figure 3b, 55.1% dispersion. These particles are well within the size range reported to be catalytically active for CO oxidation and smaller than those observed on the Au/TiO_2 reference catalysts (3.7 nm).[27] Gold XPS data collected on the freshly prepared gold catalysts show a Au_{4f} binding energy of 84.0 eV which is consistent with the formation of metallic Au^0 gold particles, Figure 4a. There was no change in the N (Figure 2) or O electronic structures measured by the XPS with the addition of gold. There was a slight increase in C−H species (284.8 eV) on the catalyst surface after catalyst preparation (4 to 15%) which could originate from hydrocarbon impurities in the vacuum deposition chamber used to prepare the gold.

Under the reaction conditions used in this study, Table 1, the equilibrium activity of the Au/TiO_2 reference catalyst was 0.17 mol CO/mol Au-sec at room temperature (24 °C) in good agreement with previously published results.[26,27] In comparison the 2.5 nm gold clusters supported on the as-prepared C_3N_4 were catalytically inactive for the gas phase oxidation of carbon monoxide at room temperature despite having smaller particles. The Au/C_3N_4 becomes catalytically active after heating to 230 °C (Figure 5). The Au/g-C_3N_4 catalysts shows thermal stability up to 500 °C in air (Figure 1b), indicating that the Au nanoparticles do not catalyze the decomposition of the support. Interestingly, unlike Au/C catalysts reported previously by Ketchie and Davis, the Au/C_3N_4 catalysts used under liquid phase conditions were also catalytically inactive under highly alkaline reaction conditions.[23]

To increase the C_3N_4's basicity the as-prepared support material was treated under alkaline conditions which has been shown on TiO_2 to result in a change in surface hydroxyl species and an increase in basicity.[14] After treating the C_3N_4 at pH 10 the support materials surface area was approximately the same, 16 m^2/g, with no microporosity, while the basicity of the carbon nitride increased to 10 from the initial pH of 6. This pH is similar to the measured pH of the Au/TiO_2 reference catalyst (pH = 9). There was no change in the C, N, and O XPS spectra (Figure 2) after treating under alkaline conditions. In addition there was no change oxygen stoichiometry as measured by the XPS and the FTIR spectra (Figure 1C,D) for the pH 10 C_3N_4 was identical to the as prepared pH 6 C_3N_4 indicating that the alkaline treatment did not result in a significant change in oxygen functionality of the support surface. However, the XPS data reveal the addition of about 0.6 at% of Na after the alkaline treatment. Additional washings of the support with warm DI water could not remove the Na. For comparison purposes the reference Au/TiO_2 catalysts has around 3 at % Na on their surfaces. There was no detectable surface chlorine.

Figure 3 (top and bottom right respectively) shows a representative STEM image and particle size histogram respectively of the gold clusters grown on the pH 10 treated C_3N_4. Similar to the gold catalyst grown on the as-prepared C_3N_4 there is a homogeneous dense distribution of gold nanoparticles with an average particle size of 2.8 nm, Figure 3 (bottom right), 50.1% dispersion. In addition, Au4f XPS data, Figure 4 (right), shows the formation of similar metallic gold species, binding energy of 84.0 eV, on the pH 10 treated C_3N_4. Similar to the gold clusters on the as prepared g-C_3N_4 there was no change in the N or O XPS data, Figure 2, and there was a 3 fold increase in C−H species (up to 11%) on the catalyst surface. Similar to the Au/C_3N_4 catalyst the Au/pH 10 C_3N_4 catalyst was inactive for the low temperature gaseous oxidation of CO. Upon heating Au on pH 10 treated g-C_3N_4 becomes active at 320 °C (Figure 5). The catalyst was also inactive for the liquid phase oxidation of CO under alkaline conditions (pH 14). For comparison purposes a gold on carbon catalyst was prepared by sputtering. A representative STEM image and particle size histogram data are shown in Supporting Information, Figures S1 and S2. The sample contained 0.66 wt % Au with average gold particles about 4.3 nm in diameter. Under liquid phase reaction conditions (pH 14, 10 psig) the

dx.doi.org/10.1021/cs3001094 | ACS Catal. 2012, 2, 1138−1146

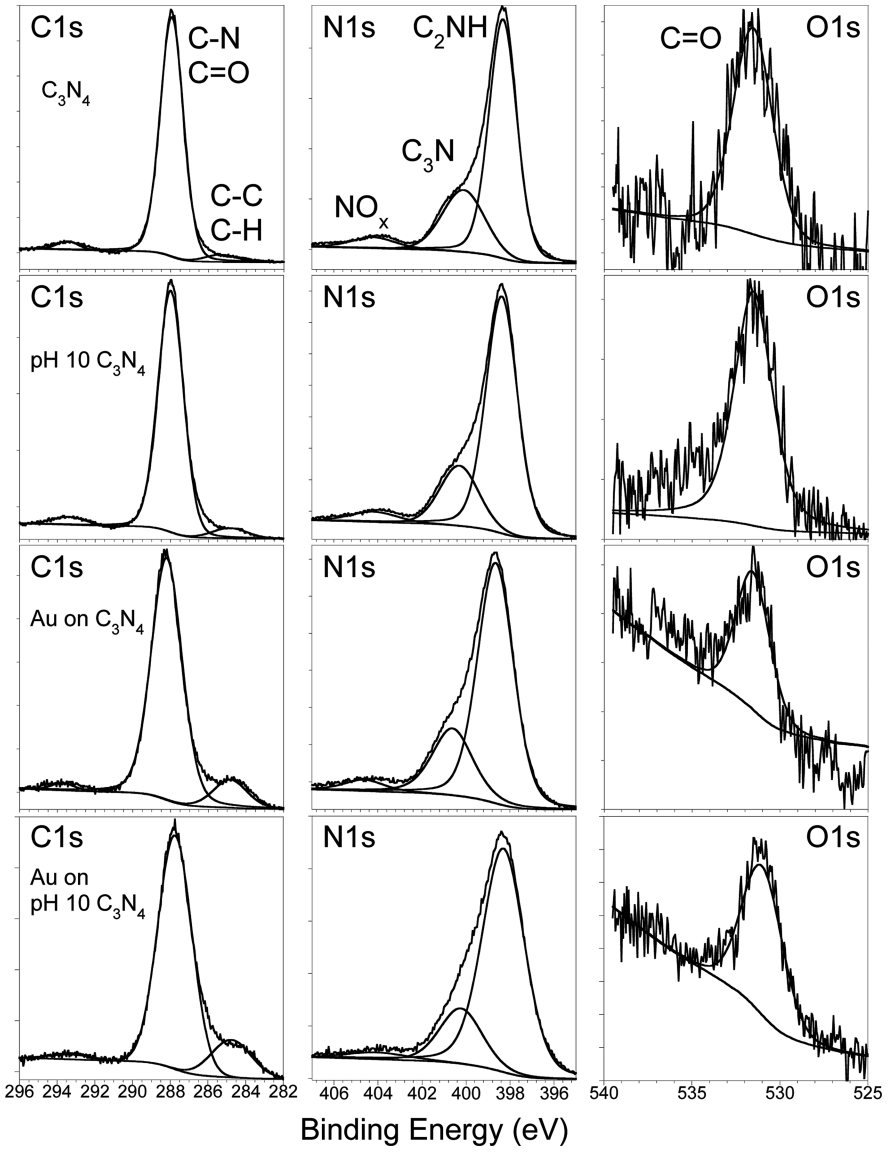

Figure 2. XPS spectra of C, N, and O regions for (top) untreated C_3N_4 prepared in N_2, (second from top) C_3N_4 after pH 10 treatment, (second from bottom) Au on C_3N_4, and (bottom) Au on pH 10 treated C_3N_4.

Table 2. Surface Functionalities Based on Peaks Fit to XPS Spectra

		Au/C_3N_4		C_3N_4		Au/C_3N_4 pH 10 treated		C_3N_4 pH 10 treated	
	functional groups	eV	%	eV	%	eV	%	eV	%
N									
	C_2NH	398.3	77	398.4	74	398.6	72	398.4	73
	N-$(C)_3$	400.2	19	400.3	21	400.6	24	400.3	22
	NO_x	404.1	3	404.3	6	404.6	4	404.2	5
O									
	C═O	530	100	530	100	530	100	530	100
C									
	C−C, C−H	284.8	15	285.0	4	284.8	11	284.9	5
	C−N, C═O	287.8	80	288.0	92	288.2	87	288.0	91
	C+	293.3	5	293.5	4	293.7	2	293.5	4

catalyst had an activity of 0.007 mol CO/mol Au·sec, Supporting Information, Figure S3.

To determine if CO binds on the Au/C_3N_4, diffuse reflectance infrared Fourier transform spectroscopy (DRIFTS) measurements were performed. A sample of Au/C_3N_4 was pretreated in He at room temperature for 1 h prior to introducing first a pulse and subsequently a steady flow of 2% CO. CO exposures were carried out at room temperature and at 263 K. Background spectra obtained prior to CO exposure showed broad features due to the C_3N_4 similar to those in

dx.doi.org/10.1021/cs3001094 | ACS Catal. 2012, 2, 1138−1146

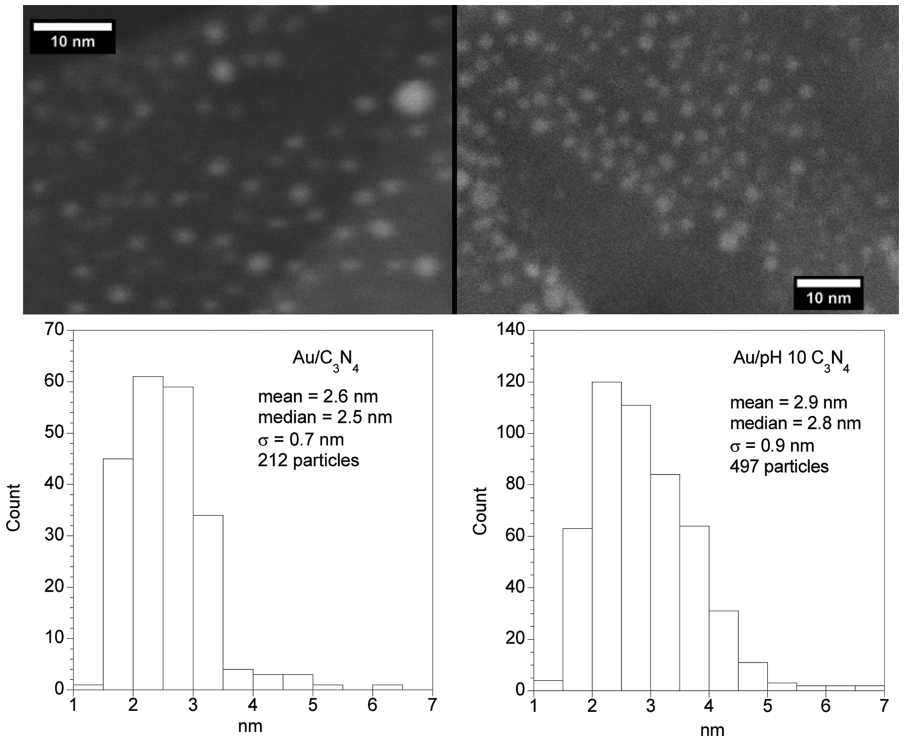

Figure 3. STEM images taken on a Hitachi HF3300 STEM operating in Z Contrast mode of (top left) Au on C_3N_4 and (top right) Au on pH 10 treated C_3N_4. Gold nanoparticles appear as bright white circles. (Lower left) Particle size histograms of gold nanoparticles on C_3N_4 and (bottom right) pH 10 treated C_3N_4.

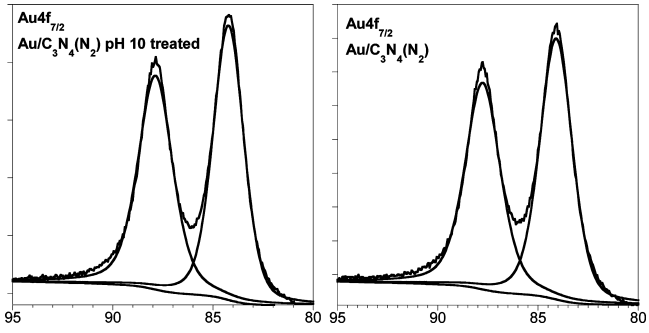

Figure 4. Au 4f XPS data for Au on C_3N_4 (left) and Au on pH 10 C_3N_4 (right) showing metallic gold species.

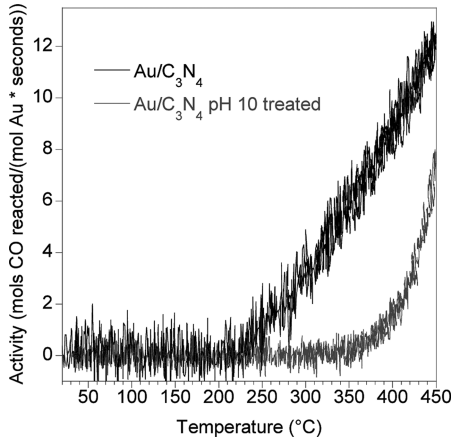

Figure 5. Catalytic Activity of gold supported on g-C_3N_4 and pH 10 treated g-C_3N_4 as a function of temperature.

Figure 1d. To look for CO adsorption pulses of gas phase CO were passed over the catalysts after pretreatment. Difference spectra showed no features typical of CO adsorption as indicated by the flat line in Figure 6d. If a continuous flow of

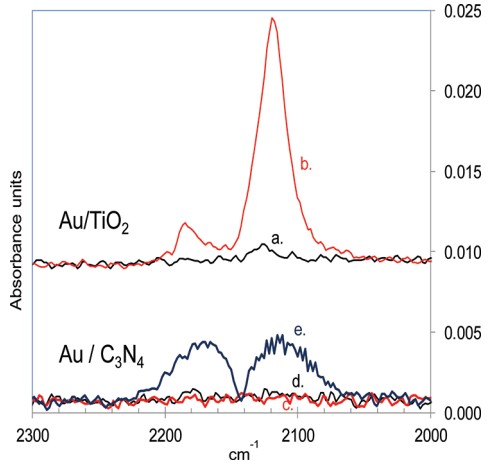

Figure 6. DRIFTS spectra in CO stretching region recorded during pulsing or flowing of 2% CO through a DRIFTS cell. For Au/TiO_2 (upper) just prior to arrival of CO pulse (curve a) and 10 s later during the pulse (curve b). For Au/C_3N_4 (lower) during CO pulse (curve c.), just prior to start of CO flow (curve d), and during continuous flow of CO pulse (e).

CO was passed across the sample, only features due to gas phase CO were observed as shown in Figure 6e. Therefore, there was no indication of adsorbed CO, even when gas phase CO is visible in the spectrum. This experiment was repeated after pretreating for 1 h in flowing He at 473 K and at 673 K,

dx.doi.org/10.1021/cs3001094 | ACS Catal. 2012, 2, 1138–1146

and also after pretreating in 4% H_2 at 673 K, but always with the same absence of stably adsorbed CO. Similarly treated C_3N_4 support also showed no CO uptake. For comparison, an experiment on prereduced Au/TiO_2 reference catalyst under similar pulsed conditions shows immediate and prominent CO adsorption at room temperature followed by rapid desorption, Figure 6.[55] Similar failure to adsorb CO has been observed for Au^{3+} species because of blocking of adsorbate sites with organic precursors;[56] however, given the evidence for Au^0 in the XPS data described above and the deposition of metallic species from a bulk metal target free of chemical precursors, it seems unlikely the lack of CO absorption is due to site blocking. The absorption of CO on Au^0 is generally believed to occur on defect sites of under coordinated gold clusters.[56] Given that the particles observed in the STEM images are around 2.5 nm it is difficult to believe that there would not be enough under-coordinated surface sites to allow a small concentration of CO to bind to the gold surface. The presence of a trace concentration of oxygen in the adsorbate gases should facilitate this absorption by promoting the oxidation of Au^0 to Au^+ in the presence of CO.[56]

DISCUSSION

We made gold catalysts on supports without surface hydroxyls to understand the influence of these strongly bound hydroxyls on the catalytic oxidation of CO by gold. The gold catalysts prepared in this work were completely inactive for the gas and liquid phase oxidation of CO and exhibit an inability to adsorb CO. The inactivity is surprising considering that the particles prepared in this study fulfill all the requirements described in the literature to obtain a catalyst with some measurable activity. Specifically, the gold particles are well within the reported size range to obtain catalytically active particles (<3.5 nm) and are smaller than those observed for the reference catalysts (3.7 nm).[2,57,58] Second, the catalysts are significantly more basic (IEP 6 and 10) than supports such as SiO_2 and WO_3 which have activities reported for catalysts prepared by sputter deposition to be 0.019 (2.5 nm)[27] and 0.002 (2.1 nm)[26] mol CO/mol Au·sec, respectively, for similarly sized gold particles at room temperature. The WO_3 used previously had a very similar surface area to the C_3N_4 used in this work, 5 m^2/g vs 13.4 m^2/g.[26] Third, the reactant gas stream is sufficiently wet (49 ppm) to obtain the maximum activity for gold catalysts supported on oxidizing and reducing supports as reported by Haruta et al.[19] Finally, the Au/C_3N_4 catalysts are completely inactive for CO oxidation under liquid phase conditions at pH 14 in NaOH. At these conditions previously inactive Au/C catalysts for gas phase CO oxidation were highly active.[22,23] A similar activity was observed for Au/C catalysts prepared by sputtering, c.f. Supporting Information, Figure S3. The lack of activity under high pH conditions is surprising since catalysts that are inactive for gas phase CO oxidation seem to react quite well in basic aqueous environments.[22,23]

Zhu et al.[59] recently reported an investigation of gold on C_3N_4 which showed that the gold catalysts were inactive for gas phase CO oxidation at temperatures below 300 °C or liquid phase oxidation of benzyl alcohol similar to our results. However, catalysts grown on activated carbon were active for these reactions under alkaline conditions.[59] These authors[59] attributed the inactivity of the C_3N_4 based catalysts to a lack of oxygen absorption/activation on vacancy sites on the support material whereas oxygen from activated carbon supports interacts with O_2 to activate it for the oxidation reaction through a defect formation/removal process.[59] The data we report above and in the literature points to a fundamentally different reason why the gold on C_3N_4 is catalytically inactive other than vacancy effects. Earlier isotope labeling studies eliminate the effect of vacancies on oxygen activation on gold catalysts.[60,61] In addition, given the small particle sizes and poor crystallinity exhibited by the C_3N_4 it is highly unlikely that there are no surface vacancies which can trap O_2 atoms to activate them.[35]

Because all the conditions required to have a gold catalyst active for a small amount of CO oxidation have been meet, that is, size, humidity, basicity, solution pH, there has to be another variable that dictates the properties of the catalyst. The most logical variable which controls activity, which has been controlled in this work, is an oxygen containing species, likely the ubiquitous OH molecule. The C_3N_4 support is unique in that it does not oxidize, according to the XPS data (Figure 1D), unlike typical nitrides (e.g., BN), and it has no OH bands evident in the FTIR data, Figure 1C. These surface hydroxyls likely mediate the activation/binding of CO molecules. Recent work by Green et al. for Au/TiO_2 may support this hypothesis.[62] Their work demonstrated the O_2 cleavage is activated by a CO-O_2 complex at the TiO_2–Au interface on gold catalysts prepared on bulk TiO_2 by deposition precipitation.[62] The CO is activated on the oxide and diffuses to the gold-oxide interface where it can react.[62] It could be that the surface OH traps the CO enabling diffusion to the gold/support interface. Without the surface OH there is no CO adsorption. This is why there is no evidence of CO absorption in the FTIR DRIFTS data.

Recent theoretical calculations confirm the importance of surface OH's in the activation of CO. These density functional theory (DFT) calculations show the addition of surface OH's to a rutile TiO_2 surface increase the binding energy of CO by about 0.75 eV and O_2 by about 0.50 eV.[63] Co-adsorption of O_2 and CO is about 0.68 eV stronger with the presence of surface OH's.[63] In addition the presence of surface OH reduces the activation barrier for CO oxidation by about 0.2 eV versus a surface without OH.[63] Similar calculations were performed for copper water gas shift catalysts and also showed the oxidation of CO by surface hydroxyls.[64]

Further evidence that surface OH's are critical is also derived from the liquid phase oxidation reaction data. If activity were solely dependent on free OH^- like what is available at pH 14 then the Au/C_3N_4 catalysts should be active like the gold nanorods and gold particles supported on carbon.[22,23] The fact that gold on carbon catalysts are inactive in the gas phase and highly active at high pH's[23] is not surprising in hindsight considering that under highly alkaline conditions high concentrations of surface OH and carboxylic acid groups are grown on the carbon surfaces[65] and probably occurred on their carbons.[23] Our data supports a mechanism where the hydroxyl species are not in solution but instead are trapped on the support surface near the gold catalyst. The well documented dependence of activity on support type parallels the strength of the basic OH sites on the metal oxides, that is, the more basic the support the more active the catalyst for CO oxidation, and is consistent with this proposed mechanism where OH groups are involved in activating the gold catalyst and the oxygen. The lack of CO adsorption on the gold clusters supported on C_3N_4 could indicate that the surface hydroxyls are required to help activate the gold to bind the CO. An envisioned mechanism is shown schematically in Figure 7.

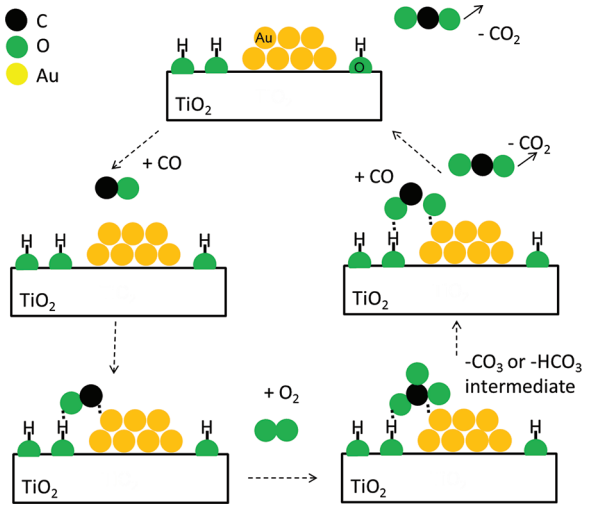

Figure 7. Schematic of envisioned reaction mechanism of CO oxidation over oxide supported gold clusters. CO interacts with surface OH and gold cluster forming "bound" CO. O_2 reacts with CO and gold at interface to form the $-CO_3$ or $-HCO_3$ intermediate. The $-CO_3$ or $-HCO_3$ intermediate decomposes releasing CO_2 while additional CO reacts with remaining oxygen from the $-CO_3$ or $-HCO_3$ intermediate and continues to form more CO_2.

CONCLUSION

In this work we report on the effect of oxygen free supports on the oxidation of carbon monoxide by supported gold nanoparticles in both the gas and the liquid phase. The inactivity of these catalysts is attributed to the lack of basic surface OH groups. These OH groups are argued to be required to activate CO for the gas phase CO oxidation.

ASSOCIATED CONTENT

Supporting Information

STEM, particle size histograms, liquid phase reactivity data for the Au/C catalysts, and proposed reaction mechanism over C_3N_4. This material is available free of charge via the Internet at http://pubs.acs.org.

AUTHOR INFORMATION

Corresponding Author

*E-mail: veithgm@ornl.gov.

Funding

A portion of this research was done using facilities at Oak Ridge National Laboratory's Center for Nanophase Materials Sciences (STEM) and at the SHaRE User Facility (TEM), which are sponsored by the Scientific User Facilities Division, Office of Basic Energy Sciences, U.S. Department of Energy. Research contributions were sponsored by the Division of Chemical Sciences, Geosciences, and Biosciences, Office of Basic Energy Sciences, U.S. Department of Energy (S.H.O. and M.L.) and by the Materials Sciences and Engineering Division, Office of Basic Energy Sciences, U.S. Department of Energy under contract with UT-Battelle, LLC (J.A.S., N.J.D., G.M.V.).

Notes

The authors declare no competing financial interest.

ACKNOWLEDGMENTS

We thank Dr. Craig Bridges for the use of the XRD and TGA, and Dr. Zhonghe Bi for the TGA measurements.

REFERENCES

(1) Kung, M. C.; Davis, R. J.; Kung, H. H. *J. Phys. Chem. C* **2007**, *111*, 11767.
(2) Haruta, M. *CATTECH* **2002**, *6*, 102.
(3) Cortie, M. B.; van der Lingen, E. *Mater. Forum* **2002**, *26*, 1.
(4) Aguilar-Guerrero, V.; Gates, B. C. *Catal. Lett.* **2009**, *130*, 108.
(5) Hartshorn, H.; Pursell, C. J.; Chandler, B. D. *J. Phys. Chem. C* **2009**, *113*, 10718.
(6) Long, C. G.; Gilbertson, J. D.; Vijayaraghavan, G.; Stevenson, K. J.; Pursell, C. J.; Chandler, B. D. *J. Am. Chem. Soc.* **2008**, *130*, 10103.
(7) Takei, T.; Okuda, I.; Bando, K. K.; Akita, T.; Haruta, M. *Chem. Phys. Lett.* **2010**, *493*, 207.
(8) Machesky, M. L.; Predota, M.; Wesolowski, D. J.; Vlcek, L.; Cummings, P. T.; Rosenqvist, J.; Ridley, M. K.; Kubicki, J. D.; Bandura, A. V.; Kumar, N.; Sofo, J. O. *Langmuir* **2008**, *24*, 12331.
(9) Mamontov, E.; Vlcek, L.; Wesolowski, D. J.; Cummings, P. T.; Rosenqvist, J.; Wang, W.; Cole, D. R.; Anovitz, L. M.; Gasparovic, G. *Phys. Rev. E* **2009**, 79.
(10) Mamontov, E.; Vlcek, L.; Wesolowski, D. J.; Cummings, P. T.; Wang, W.; Anovitz, L. M.; Rosenqvist, J.; Brown, C. M.; Sakai, V. G. *J. Phys. Chem. C* **2007**, *111*, 4328.
(11) Mamontov, E.; Wesolowski, D. J.; Vlcek, L.; Cummings, P. T.; Rosenqvist, J.; Wang, W.; Cole, D. R. *J. Phys. Chem. C* **2008**, *112*, 12334.
(12) Zhang, Z.; Fenter, P.; Sturchio, N. C.; Bedzyk, M. J.; Machesky, M. L.; Wesolowski, D. J. *Surf. Sci.* **2007**, *601*, 1129.
(13) Henderson, M. A. *Surf. Sci. Rep.* **2002**, *46*, 1.
(14) Veith, G. M.; Lupini, A. R.; Dudney, N. J. *J. Phys. Chem. C* **2009**, *113*, 269.
(15) Li, S.-C.; Diebold, U. *J. Am. Chem. Soc.* **2009**, *132*, 64.
(16) Bond, G.; Thompson, D. *Gold Bull.* **2009**, *42*, 247.
(17) Cunningham, D. A. H.; Kobayashi, T.; Kamijo, N.; Haruta, M. *Catal. Lett.* **1994**, *25*, 257.
(18) Daté, M.; Ichihashi, Y.; Yamashita, T.; Chiorino, A.; Boccuzzi, F.; Haruta, M. *Catal. Today* **2002**, *72*, 89.
(19) Daté, M.; Okumura, M.; Tsubota, S.; Haruta, M. *Angew. Chem., Int. Ed.* **2004**, *43*, 2129.
(20) Calla, J. T.; Davis, R. J. *Ind. Eng. Chem. Res.* **2005**, *44*, 5403.
(21) Costello, C. K.; Yang, J. H.; Law, H. Y.; Wang, Y.; Lin, J. N.; Marks, L. D.; Kung, M. C.; Kung, H. H. *Appl. Catal., A* **2003**, *243*, 15.
(22) Sanchez-Castillo, M. A.; Couto, C.; Kim, W. B.; Dumesic, J. A. *Angew. Chem., Int. Ed.* **2004**, *43*, 1140.
(23) Ketchie, W. C.; Murayama, M.; Davis, R. J. *Top. Catal.* **2007**, *44*, 307.
(24) Moreau, F.; Bond, G. C.; van der Linden, B.; Silberova, B. A. A.; Makkee, M. *Appl. Catal., A* **2008**, *347*, 208.
(25) Haruta, M. *J. New Mater. Electrochem. Syst.* **2004**, *7*, 163.
(26) Veith, G. M.; Lupini, A. R.; Pennycook, S. J.; Villa, A.; Prati, L.; Dudney, N. J. *Catal. Today* **2007**, *122*, 248.
(27) Veith, G. M.; Lupini, A. R.; Rashkeev, S. N.; Pennycook, S. J.; Mullins, D. R.; Schwartz, V.; Bridges, C. A.; Dudney, N. J. *J. Catal.* **2009**, *262*, 92.
(28) Veith, G. M.; Lupini, A. R.; Pennycook, S. J.; Dudney, N. J. *ChemCatChem* **2010**, *2*, 281.
(29) Edwards, J. K.; Ntainjua, N, E.; Carley, A. F.; Herzing, A. A.; Kiely, C. J.; Hutchings, G. J. *Angew. Chem., Int. Ed.* **2009**, *48*, 8512.
(30) Qian, K.; Zhang, W.; Sun, H.; Fang, J.; He, B.; Ma, Y.; Jiang, Z.; Wei, S.; Yang, J.; Huang, W. *J. Catal.* **2011**, *277*, 95.
(31) Jiang, D.-e.; Overbury, S. H.; Dai, S. *J. Phys. Chem. Lett.* **2011**, *2*, 1211.
(32) Zhao, K.; Qiao, B.; Wang, J.; Zhang, Y.; Zhang, T. *Chem. Commun.* **2011**, *47*, 1779.
(33) Brown, M. A.; Carrasco, E.; Sterrer, M.; Freund, H. J. *J. Am. Chem. Soc.* **2010**, *132*, 4064.
(34) Goettmann, F.; Thomas, A.; Antonietti, M. *Angew. Chem., Int. Ed.* **2007**, *46*, 2717.
(35) Thomas, A.; Fischer, A.; Goettmann, F.; Antonietti, M.; Muller, J. O.; Schlogl, R.; Carlsson, J. M. *J. Mater. Chem.* **2008**, *18*, 4893.

(36) Onodera, T.; Suzuki, S.; Mizukami, T.; Kanzaki, H. *J. Power Sources* **2011**, *196*, 7994.
(37) Byon, H. R.; Suntivich, J.; Shao-Horn, Y. *Chem. Mater.* **2011**, *21*, 3421.
(38) Wang, Y.; Wang, X.; Antonietti, M. *Angew. Chem., Int. Ed.* **2011**, *51*, 68.
(39) Kaukonen, M.; Kujala, R.; Kauppinen, E. *J. Phys. Chem. C* **2011**, *116*, 632.
(40) Bredow, T.; Pacchioni, G. *Chem. Phys. Lett.* **2002**, *355*, 417.
(41) Vijay, A.; Mills, G.; Metiu, H. *J. Chem. Phys.* **2003**, *118*, 6536.
(42) Wang, L.-Q.; Baer, D. R.; Engelhard, M. H. *Surf. Sci.* **1994**, *320*, 295.
(43) Veith, G. M.; Lupini, A. R.; Pennycook, S. J.; Dudney, N. J. In *Studies in Surface Science and Catalysis*; Gaigneaux, E., Devillers, M., De Vos, D. E., Hermans, S., Jacobs, P. A., Martens, J. A., Ruiz, P., Eds.; Elsevier: Amsterdam, The Netherlands, 2006; Vol. *162*, p 71.
(44) Abramoff, M. D.; Magelhaes, P. J.; Ram, S. J. *Biophotonics Int.* **2004**, *11*, 36.
(45) Maeda, K.; Domen, K. *J. Phys. Chem. C* **2007**, *111*, 7851.
(46) Wang, X. C.; Maeda, K.; Thomas, A.; Takanabe, K.; Xin, G.; Carlsson, J. M.; Domen, K.; Antonietti, M. *Nat. Mater.* **2009**, *8*, 76.
(47) Groenewolt, M.; Antonietti, M. *Adv. Mater.* **2005**, *17*, 1789.
(48) Cullity, B. D. *Elements of X-ray Diffraction* 2nd ed.; Addison-Wesley Publishing Company, Inc.: Reading, MA, 1978.
(49) Niewa, R.; DiSalvo, F. J. *Chem. Mater.* **1998**, *10*, 2733.
(50) Li, Q.; Yue, B.; Iwai, H.; Kako, T.; Ye, J. *J. Phys. Chem. C* **2010**, *114*, 4100.
(51) Montigaud, H.; Tanguy, B.; Demazeau, G.; Alves, I.; Courjault, S. *J. Mater. Sci.* **2000**, *35*, 2547.
(52) Guo, Q.; Xie, Y.; Wang, X.; Zhang, S.; Lv, S. *Chem. Commun.* **2004**, 26.
(53) Lotsch, B. V.; Doblinger, M.; Sehnert, J.; Seyfarth, L.; Senker, J.; Oeckler, O.; Schnick, W. *Chem.—Eur. J.* **2007**, *13*, 4969.
(54) Kundu, S.; Wang, Y.; Xia, W.; Muhler, M. *J. Phys. Chem. C* **2008**, *112*, 16869.
(55) Clark, J. C.; Dai, S.; Overbury, S. H. *Catal. Today* **2007**, *123*, 135.
(56) Mihaylov, M.; Knozinger, H.; Hadjiivanov, K.; Gates, B. C. *Chem. Ing. Tech.* **2007**, *79*, 795.
(57) Haruta, M. *Catal. Today* **1997**, *36*, 153.
(58) Valden, M.; Lai, X.; Goodman, D. W. *Science* **1998**, *281*, 1647.
(59) Zhu, J.; Carabineiro, S. A. C.; Shan, D.; Faria, J. L.; Zhu, Y.; Figueiredo, J. L. *J. Catal.* **2010**, *274*, 207.
(60) Calla, J. T.; Davis, R. J. *J. Phys. Chem. B* **2005**, *109*, 2307.
(61) Calla, J. T.; Davis, R. J. *J. Catal.* **2006**, *2*, 407.
(62) Green, I. X.; Tang, W.; Neurock, M.; Yates, J. T. *Science* **2011**, *333*, 736.
(63) Ganesh, P.; Kent, P. R. C.; Veith, G. M. *J. Phys. Chem. Lett.* **2011**, *2*, 2918.
(64) Gokhale, A. A.; Dumesic, J. A.; Mavrikakis, M. *J. Am. Chem. Soc.* **2008**, *130*, 1402.
(65) Li, Q.; Lueking, A. D. *J. Phys. Chem. C* **2011**, *115*, 4273.